A Model for Antiplasticization in Polystyrene

S. L. Anderson,[†] E. A. Grulke,*[,†] P. T. DeLassus,[†,‡] P. B. Smith,[‡] C. W. Kocher,[‡] and B. G. Landes[‡]

Chemical Engineering Department, Michigan State University, East Lansing, Michigan 48824-1226, and The Dow Chemical Company, Midland, Michigan 48667

Received August 9, 1993; Revised Manuscript Received July 20, 1994[⊗]

ABSTRACT: Antiplasticization can occur when small quantities of a known "plasticizer" have been blended into a glassy polymer. Commonly, the T_g of the polymer and its free volume decrease. However, the mechanical properties of the antiplasticized polymer are altered significantly, causing the polymer to become stiffer and more brittle. Experimental results from flexural tests of polystyrene/mineral oil blends conducted at room temperature showed that antiplasticization is molecular weight dependent, thus supporting a hypothesis that the phenomenon can be attributed to a chain-end effect. A high molecular weight polystyrene (M_w = 270 000 D) exhibited plasticization only, whereas a low molecular weight (M_w = 40 000 D) exhibited both antiplasticization and plasticization effects. The 40 000 MW sample showed a 2-fold increase in flexural moduli and flexural strengths as mineral oil concentration increased up to 6 vol %. These moduli and strengths decreased rapidly at higher concentrations of mineral oil. Positron annihilation spectroscopy (PAS) data showed a 10% decrease in fractional free volume up to 6% mineral oil. ^{13}C NMR experiments showed that there was no change in the polymer backbone dynamics during antiplasticization. ^{1}H NMR Goldman−Shen experiments showed that antiplasticization occurs when the average diameter of the mineral oil domains is less than the average size of the free volume voids. It was determined that one mineral oil molecule was associated with a polystyrene chain end during antiplasticization. These results are consistent with the hypothesis that antiplasticization is due to a decrease in fractional free volume at the chain ends.

Introduction

In the past 25 years, there has been documented evidence of antiplasticization, an unusual phenomenon that occurs when small quantities of a known "plasticizer" have been blended into a glassy polymer.[1,2] Although the glass transition temperature (T_g) of a polymer may be lowered upon addition of these plasticizers, the modulus and tensile strength increase significantly, causing the polymer to become stiffer and more brittle. This behavior is opposite to that expected of a plasticized material—the material behaves as though motions in the polymer chains are restricted. In addition, the transport properties are affected.[3]

Antiplasticization has been observed in many polymer−diluent systems, e.g., polycarbonate and dibutyl phthalate, poly(vinyl chloride) and tricresyl phosphate, and nylon and water. Mechanical property tests, differential scanning calorimetry (DSC), dynamic mechanical spectroscopy (DMS), dielectric loss studies, nuclear magnetic resonance (NMR), and density measurements collectively infer that antiplasticization results from one or more of the following: (a) a decrease in free volume upon the addition of the diluent—perhaps the polymer chains have some small degree of mobility which allows them to align themselves in a more ordered densely packed state or that the diluents fill the excess volume of the polymer glass;[3,4] (b) suppression of the secondary relaxation transitions at the temperature of interest;[5] (c) polymer−diluent interactions which create steric hindrance and decrease segmental mobility of the polymer;[5,6] (d) reduced mobility of the diluent—perhaps solid diluents with higher glass transition temperatures near the temperature of mechanical testing have a greater tendency to promote antiplasticization.[4]

Most previous work[1−16] has relied solely on either a mechanical or an analytical test to verify antiplasticization and then speculated on a mechanism for antiplasticization. No one has related the microscopic physical behavior of the diluent to the local molecular motions of the polymer and then extended that information to explain the bulk mechanical behavior of the polymer.

The most predominant hypothesis given for antiplasticization is that it is due to hole-filling by the diluent and hence results in a decrease in the free volume of the polymer. Attributing antiplasticization to a decrease in free volume was based, until now, solely on density measurements and theoretical calculations. There is no prior published report which describes the hole-filling mechanism of the diluent. The purpose of this paper is to study the hole-filling mechanism and propose a model for antiplasticization.

Polystyrene/mineral oil blends were studied as a model system. The experimental approach is to measure directly the changes in free volume, hole sizes and hole number densities using PAS and then relate those results to polymer chain dynamics data obtained via solid-state NMR techniques.

Experimental Approach

Flexural Properties. Flexural mechanical tests of rectangular bars were conducted, instead of tensile tests, due to the brittle nature of the polystyrene/mineral oil blends. The three-point bending technique was used in accordance with ASTM Method D-790 procedures.[17] The flexural strength is calculated using the maximum load at which there is no longer an increase in load with increasing deflection.[18,19]

[†] Michigan State University.
[‡] The Dow Chemical Co.
[⊗] Abstract published in *Advance ACS Abstracts,* March 1, 1995.

0024-9297/95/2228-2944$09.00/0

Positron Annihilation Spectroscopy. Positron annihilation spectroscopy (PAS) was used to determine changes in free volume. This procedure is a valuable tool for studying defects/holes in solids. It relies on the affinity of orthopositronium (o-Ps) for domains with low electron densities. Information about o-Ps lifetimes and intensities can be used to calculate the average hole size and hole number densities.[20]

Positrons with high energy are emitted from a radioactive isotope such as ^{22}Na and thermalize quickly upon entering a condensed sample. They can exist in several states, each having a characteristic lifetime τ_i and intensity I_i. Typically, PAS spectra are resolved into three exponentially decaying components corresponding to the specific state of the positron. Positrons may annihilate with free electrons in condensed media, resulting in photon emission. A positron may also combine with an electron to form a positronium (Ps), which can exist in either the singlet i.e., para, state, or triplet, i.e., ortho, state, depending on the spin state of the bound electron. Parapositronium (p-Ps) has the shortest lifetime of about 0.1 ns, corresponding to τ_1. In condensed media free positrons and positron–molecular complexes have intermediate lifetimes of about 0.4–0.8 ns, corresponding to τ_2. The longest lifetime component, τ_3 of 1–10 ns, attributed to orthopositronium (o-Ps) "pick-off decay" by electrons, is used to study free volume changes. The o-Ps lifetime, τ_3, is proportional to the average hole size, while the intensity, I_3, of the o-Ps component of the lifetime spectra is proportional to the number density of holes. An approximate measure of the relative free volume can be obtained from the product of the lifetime and the relative intensity.

Determination of Average Hole Size from PAS Lifetimes. Tao and Nakanishi, using the particle-in-a-spherical-box theory, have shown that that the o-Ps lifetime, τ_3, can be related to the average hole radius, r, in the following way.[21,22]

$$\tau_3 = 0.5\left(1 - \frac{r}{r + 0.166} + 0.159 \sin\left(\frac{2\pi r}{r + 0.166}\right)\right)^{-1} \quad (1)$$

Several researchers have observed excellent agreement between measured o-Ps lifetimes and average hole radii for materials with known hole sizes.[22] The average hole volume, $\langle V \rangle$, is then derived from

$$\langle V \rangle = \frac{4\pi r^3}{3} \quad (2)$$

Determination of Fractional Free Volume and Number Density of Holes. Brandt et al. have shown that the o-Ps intensity, I_3, is a measure of the number density of holes or free volume sites.[23] Given that $n(v)$ dv is the number density of holes having volumes between v and $(v + dv)$, then the number of holes per unit volume, N, is the integral, $\int n(v)\, dv$.

The fractional free volume, f_v, is given as

$$f_v = \int n(v) v \, dv = \langle V \rangle N \quad (3)$$

$$f_v = c\langle V \rangle I_3, \quad \text{where } N = cI_3 \quad (4)$$

The parameter c is a proportionality constant relating o-Ps intensity, I_3, to the total number density of holes, N. The constant c, which depends on the type of polymer, can be determined from a calculated or known value of the fractional free volume of pure polystyrene.

The free volume, V_f, of a polymer at any temperature T is typically explained as the difference between the specific volume of the polymer, V_T, and the specific volume of the equilibrium liquid or occupied volume, V_0, at 0 K.

$$V_f = V_T - V_0 \quad (5)$$

According to Bondi,[24] $V_0 \approx 1.3V_w$, where V_w is the van der Waals specific volume determined from group contributions. The fractional free volume of the polymer is given by

$$f_V = \frac{V_f}{V_T} = \frac{V_T - V_0}{V_T} \quad (6)$$

$$V_T = V_{273K} \exp(\alpha_g (T - 273)) \quad (7)$$

where $\alpha_g = d \ln V/dT$ is the coefficient of thermal expansion of the glass at constant pressure.

Nuclear Magnetic Resonance. Three relaxation times are used to characterize the relaxation of nuclear spins in NMR experiments.[25] These are T_1, the spin–lattice relaxation time, T_2, the spin–spin relaxation time, and $T_{1\varrho}$, the spin–lattice relaxation time in the rotating frame. $T_{1\varrho}$, which describes molecular dynamics on the kilohertz scale, is used to characterize polymer dynamics. Since these polymer motions are slower than the NMR frequency or Larmor frequency, an increase in $T_{1\varrho}$ indicates a decrease in the relaxation rate. In more mobile systems such as low-viscosity liquids, an increase in T_1 or $T_{1\varrho}$ indicates faster molecular motions.

Magic angle spinning (MAS) and cross-polarization (CP) make it possible to overcome the resolution and sensitivity enhancement problems of the signal in solid-state NMR experiments.[26–28] MAS spins the sample at 54.7° with respect to the direction of the applied magnetic field, averaging all anisotropic interactions such as dipole–dipole couplings which would otherwise cause significant NMR line broadening.[27] In CP experiments, 90° pulses are applied separately to the ^{1}H and ^{13}C spins along the Y axis, with spin-locking, allowing them to precess in the XY plane, for a given contact time, T_c. The polarization of the ^{13}C spins is increased, which increases their sensitivity. Magnetization is transferred from the ^{1}H coupled to the ^{13}C at a time constant, T_{C-H}, which is the time constant for the buildup of the ^{13}C signal.[28]

The intensity, I, of the ^{13}C signal depends on T_{C-H} and ^{1}H $T_{1\varrho}$ according to the following equation:

$$I(t) = I_0\left[\left(1 - \frac{T_{C-H}}{T_{1\varrho}(H)}\right) \times \left(\exp\left(\frac{-T_c}{T_{1\varrho}(H)}\right) - \exp\left(-\left(\frac{T_c}{T_{C-H}}\right)\right)\right)\right] - 1 \quad (8)$$

Studies of domain sizes in polymers can be conducted via ^{1}H NMR experiments since mobile domains exhibit significantly different T_2 relaxation times when compared to rigid domains.

A Goldman–Shen pulse sequence

$$\left(\left(\frac{\pi}{2}\right)_x - t_0 - \left(\frac{\pi}{2}\right)_x - t - \left(\frac{\pi}{2}\right)_x\right)$$

is applied to destroy selectively the magnetization of the rigid domains.[29,30] This facilitates the transfer of mag-

netization from the mobile to the rigid domains. By monitoring the recovery of magnetization in the rigid domains, one can determine the size and shape of the mobile domains from the following equations.

$$R(t) = \frac{M(t)}{M(t\rightarrow\infty)} \tag{9}$$

$$R(t) = 1 - \frac{1}{\exp(Dt/b^2)} \tag{10}$$

$$D = 0.13\frac{a^2}{T_2} \tag{11}$$

where $M(t)$ is the magnetization in the rigid phase, $R(t)$ is the recovery factor, D is the spin diffusion coefficient in the rigid domain, b is the mobile domain size, a is the H−H bond distance = 0.2 nm, and T_2 is the spin−spin relaxation time.

Experimental Section

Materials and Blending. Three different types of atactic polystyrene (M_w = 270 000 and 40 000 Da, obtained from Scientific Polymer Products, Inc., and a 128 000 MW sample obtained from The Dow Chemical Co.) were blended separately with different concentrations of Penreco Drakeol Supreme High Viscosity mineral oil in a Haake Buchler Rheocord System 40 mixing bowl set at 50 rpm and 200 °C. Nominal mineral oil concentrations of 0−10 parts per hundred resin (0−9.09 wt % or 0−10.9 vol %) were studied. The sample with an average molecular weight of 40 000 actually had a bimodal distribution, as shown in Table 1 of the results section. On a number-average basis, this material would be similar to a 50:50 blend of the 128 000 molecular weight sample with polystyrene oligomers having about nine repeating units per chain. The number of chain ends per gram of this material was 1.19×10^{-3}. Adding mineral oil to this material resulted in an increase in the chain ends per gram of sample, since the mineral oil molecular weight is less than that of the low molecular weight fraction of the polystyrene. Therefore, antiplasticization effects observed in the melt or solid states for this polymer sample mixed with mineral oil could not be attributed to a decrease in chain ends per gram.

Gel Permeation Chromatography (GPC). Molecular weight distributions of the pure polystyrene samples, dissolved in HPLC grade tetrahydrofuran (THF) with 500 ppm di-*tert*-butylbenzene as an internal standard, were determined using a Hewlett-Packard GPC. The instrument was calibrated using 12 narrow anionic polystyrene standards (MW = 2.95×10^6 to 2.2×10^3) obtained from Polymer Laboratories, Inc. Two PLgel Sum mixed columns (each 7.5 mm × 300 mm), obtained from Polymer Laboratories, were used in series at 40 °C to obtain separation. The injection sample volume was 50 mL of 0.25% polymer solution in THF eluent. The flow rate of the THF eluent was 1 mL/min. The samples were filtered prior to injection. A filter photometric detector tuned to 254 nm was used. The support apparatus consisted of a Hewlett-Packard 1090 liquid chromatograph with autosampler, an HP 85−B computer, and a 9153A controller.

Gas Chromatography. High-temperature gas chromatography (GC) with flame ionization detection and a Quadrex aluminum-clad capillary column (25 m × 0.25 mm i.d., 0.1 mm) with split injection was used to determine the qualitative nature of the mineral oil. The temperature ramp was from 100 to 400 °C. The chromatogram of the mineral oil was compared to a chromatogram of a mixture of C-7 to C-40 straight-chain hydrocarbons obtained from Polysciences Corp. (Analytical Standard Kit 21c and 26 cx).

Compression Molding. Compression bars (approximately 0.076 × 0.012 × 0.0016 m or 3 × 1/2 × 1/16 in.) were molded in an electrically heated hydraulic press set at 200 °C and 3000 psi for 3 min.

Mineral Oil Concentrations. The mineral oil concentration in the molded bars was determined by gas chromatography (GC) using polystyrene samples dissolved in methylene chloride. The analyses were performed with a Waters 510 HPLC pump, a Spectrum 1021A filter and amplifier, an ACS Model 750/14 mass detector, and a Hewlett-Packard 3396A integrator. A DuPont ZORBAX SIL 4.6 mm × 25 cm column with a Brownlee Labs silica 4.6 mm × 3 cm guard column was used. HPLC grade hexane was the mobile phase. The injection size was 20 μL. The flow rate was 1.5 mL/min. The analyses were conducted at room temperature. Standardization was accomplished using standards containing 0.5−10 wt % mineral oil dissolved in methylene chloride.

Table 1. Molecular Weight Distribution of Polystyrenes

	270 000 MW	128 000 MW	bimodal 40 000 MW	
M_n	111 700	58 420	56 970	850
M_w	274 400	127 900	103 900	1 058
M_z	448 100	216 400	164 700	1 343
M_p	244 200	87 930	109 300	751
PD[a]	2.455	2.190	1.824	1.245

[a] PD = polydispersity.

Differential Scanning Calorimetry. Glass transition temperatures of the blends (after molding) were determined by differential scanning calorimetry using a DuPont 9900 computer/thermal analyzer calibrated with an indium reference standard. Scanning rates were 10 °C/min from room temperature to 200 °C. All samples were run in air.

Flexural Properties. Flexural moduli and flexural strengths of the compression-molded bars were determined at room temperature using an Instron Model 4201 universal testing instrument. The tests were done at room temperature a few days after molding according to ASTM Method D790 for a three-point bend test. Tensile property testing could not be performed due to the extremely brittle nature of these bars.

Positron Annihilation Spectroscopy. PAS experiments were conducted at 23 °C in air using a ^{22}Na source (50 μCi) deposited on a 0.1 mil thick Mylar film and sandwiched between two layers (each approximately 1 mm thick) of compression-molded, 1 in. diameter polystyrene sample disks. PAS spectra were acquired using a standard fast−fast coincidence spectrometer from EG&G Ortec. The birth γ and annihilation γ rays were detected by two detectors, one set at 1.28 MeV and the other set at 0.511 MeV energy, respectively. Each detector consisted of a photomultiplier (RCA 8835) and a fast plastic scintillator (Pilot U). Approximately 3 million counts were accumulated during an 8 h period. The lifetime spectra were resolved into three exponentially decaying components using PCPFIT, which is a PC version of POSITRONFIT EXTENDED.[31]

Nuclear Magnetic Resonance. The blend samples were ground in a mortar and loaded into 4 mm zirconium rotors. The analysis was done using a Bruker MSL-200 NMR spectrometer. Cross-polarization, magic angle spinning ^{13}C NMR spectroscopy was performed at 50.3 MHz using a 4 mm rotor and spinning at about 7 kHz. The relaxation delay was 8 s, the proton 90° pulse width was 6 ms, the contact time was 1 ms, the acquisition time was 80 ms, the sweep width was 20 kHz, the data size was 8K, and the apodization was exponential with 10 Hz line broadening.

^{13}C NMR $T_{1\rho}$ values were determined in the conventional way.[28] T_{CH} and ^{1}H $T_{1\rho}$ values were determined from contact time experiments.

Goldman−Shen spin diffusion experiments were conducted to determine the domain sizes of the mineral oil.[29,30] The experiments were performed using the same spectrometer at 200.14 MHz for ^{1}H NMR. The relaxation delay was 8 s, the proton 90° pulse width was 6 ms, the acquisition time was 80 ms, the sweep width was 200 kHz, the data size was 4K, and the apodization was exponential with 10 Hz line broadening. The delay between the first two 90° pulses to allow the T_2 relaxation of the rigid polystyrene phase was 200 s.

Results and Discussion

Molecular Weight Distribution of the Polystyrene Samples. The molecular weight distributions for the polystyrene samples are shown in Table 1. The

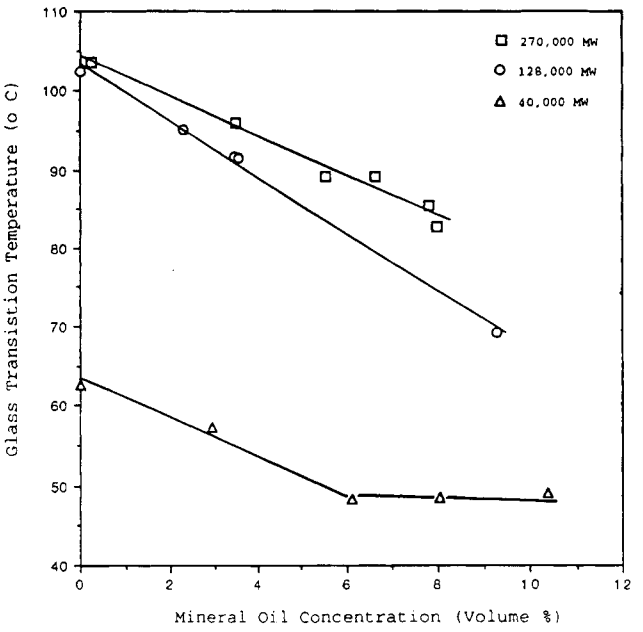

Figure 1. Effect of mineral oil concentration on T_g.

40 000 MW sample was bimodal. All of these materials were synthesized by free-radical polymerization.

Gas Chromatogram of the Mineral Oil. The high-temperature gas chromatogram indicated that the mineral oil sample was comprised of primarily C-28 to C-46 hydrocarbons.

Solubility of Mineral Oil in Polystyrene. GC analysis of the 270 000 MW, 128 000 MW, and 40 000 MW polystyrene test bars indicated a maximum concentration of approximately 8, 9, and 10 vol % of absorbed mineral oil, respectively, compared to the nominal 11% concentration that was added to the polystyrene in the Haake mixing bowl. Blends containing >8% mineral oil were opaque at room temperature; i.e., phase separation occurred as temperature was decreased. This was indicative of upper critical solution temperature (UCST) behavior.

Glass Transition Temperatures. Figure 1 shows that the glass transition temperatures decreased with mineral oil concentration. There was a 25 and a 15 °C decrease in glass transition temperatures for the 270 000 and 40 000 molecular weight blends, respectively, at the highest mineral oil concentrations. While the T_g of the 270 000 MW blends decreased linearly, there was a change in slope in the T_g of the 40 000 MW blends at 6% mineral oil. At concentrations <6% mineral oil, the T_g decreased linearly, whereas above 6% mineral oil, the T_g of the 40 000 MW blends remained constant. This change in slope at 6% corresponds to the work of Braun et al. and Pezzin et al., where they describe a singularity in the T_g versus concentration data of poly(vinyl chloride) with dibutyl phthalate and dicyclohexyl phthalate.[32,33] This singularity occurs when the diluent eliminates the WLF free volume. According to Boyer, the plasticizer is more efficient at lowering the free volume once this singularity is achieved.[34] A similar deviation in T_g from linearity was observed by Cais et al. with polycarbonate–diluent blends.[16]

Flexural Properties of Polystyrene/Mineral Oil Blends. Figure 2 illustrates the effect of mineral oil concentration on the flexural properties of the 270 000 MW polystyrene blends. As commonly observed with polystyrene, the flexural modulus of the 270 000 MW materials decreased significantly only at concentrations greater than 5%, whereas there was an immediate

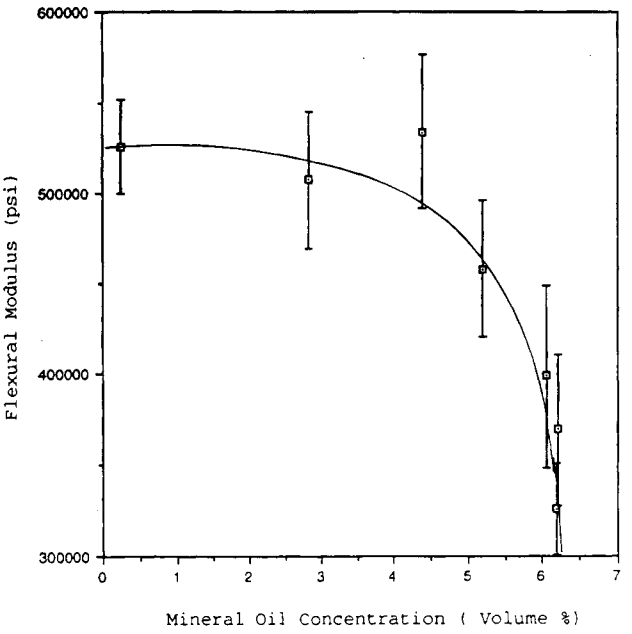

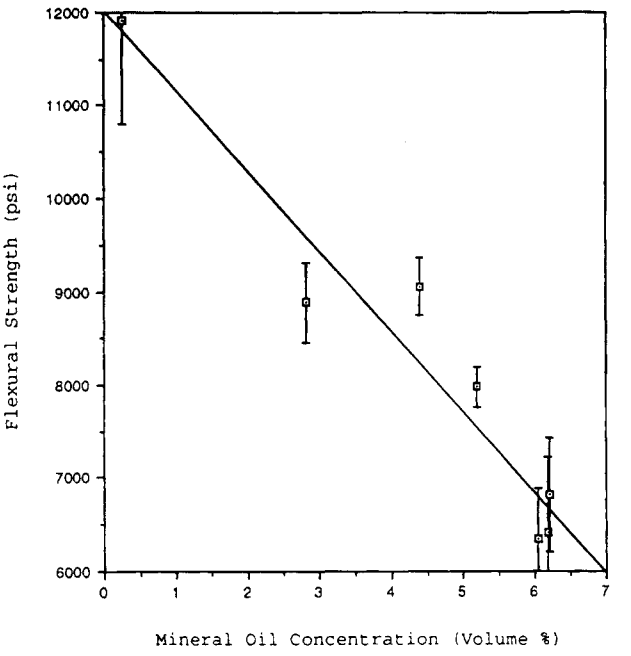

Figure 2. Effect of mineral oil concentration on flexural modulus of 270 000 MW blends.

decrease in flexural strength as mineral oil was added to the system. This was indicative of plasticization of the high molecular weight polystyrene by the mineral oil. The error bars on the graphs represent a 95% confidence interval.

Figure 3 shows the effect of the mineral oil concentration on the flexural properties of the 40 000 MW polystyrene blends. There was approximately a 2-fold increase in flexural modulus up to about 6% mineral concentration, followed by a rapid decrease in flexural modulus with higher concentrations of mineral oil. The same behavior was seen with the flexural strength. There was a 1.7-fold increase in flexural strength up to about 8% mineral oil concentration followed by a rapid drop in flexural strength at higher mineral oil concentrations. The increase in flexural modulus and strength is indicative of antiplasticization. This apparent stiffening of the blend below T_g resulted when small quantities of mineral oil (<6%) were blended into 40 000 MW atactic polystyrene. This behavior was not observed in

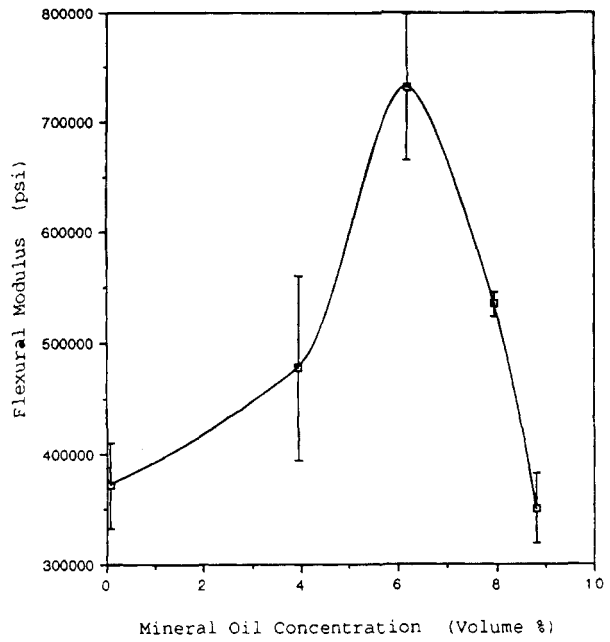

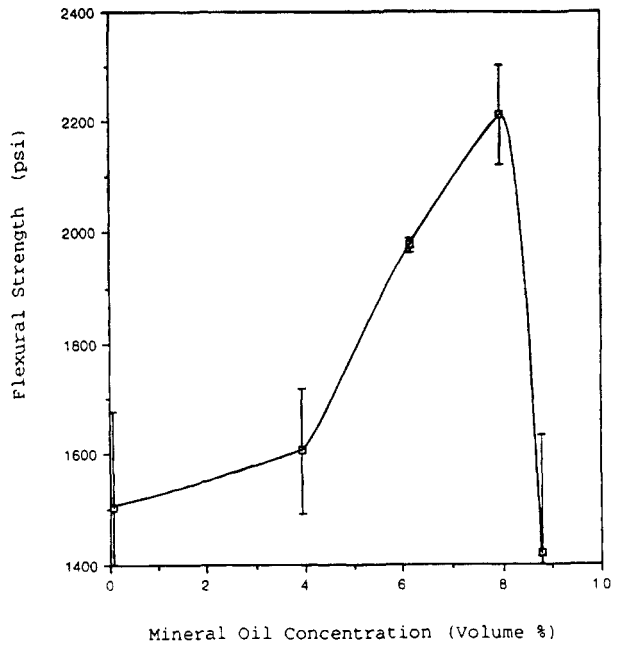

Figure 3. Effect of mineral oil concentration on flexural modulus of 40 000 MW blends.

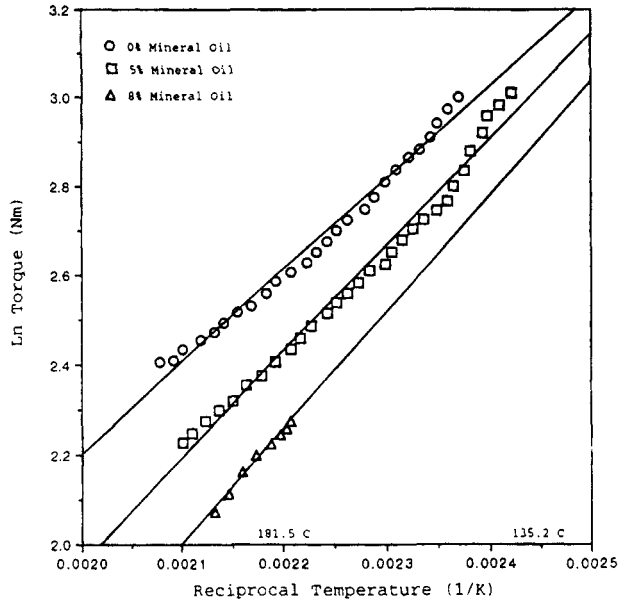

Figure 4. Effect of mineral oil concentration on torque of 270 000 MW blends.

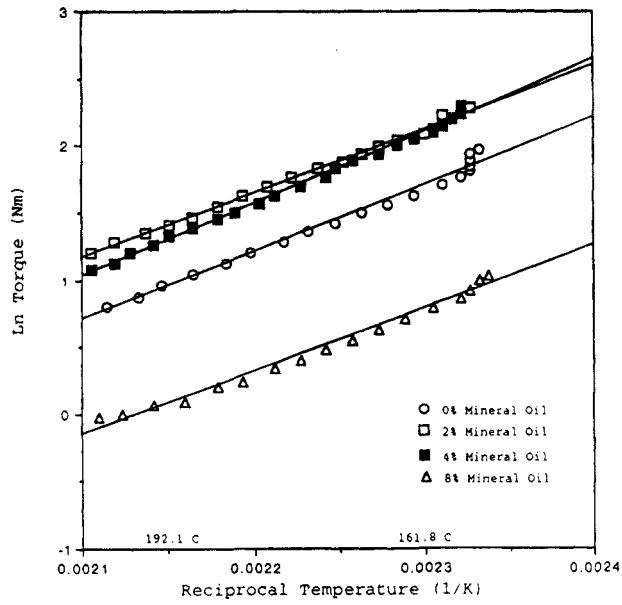

Figure 5. Effect of mineral oil concentration on torque of 128 000 MW blends.

the 270 000 MW polystyrene blends. Possibly antiplasticization occurs only below a critical molecular weight. These results directly support the hypothesis that antiplasticization is primarily attributed to a chain end effect.

The 40 000 MW bimodal sample had a significantly greater concentration of chain ends than the 270 000 MW material. Using a basis of 1 000 000 g, one determines that the 270 000 MW sample had approximately 18 mol of chains ends, whereas the 40 000 MW bimodal sample had 1426 mol (14 and 1412 mol for the high and low molecular weight fractions, respectively). There are two orders of magnitude more "voids" available at the chain ends in the low molecular weight material for the mineral oil to occupy and hinder the mobility and realignment of the polymer chain.

Behavior of Polystyrene Blends above T_g. Torque data at different temperatures were collected for these materials after homogeneity was achieved in the Haake mixing bowl. Figures 4–6 show the Arrhenius plot of ln(torque) versus reciprocal temperature for the different blends.

As expected the 270 000 MW blends showed a decrease in torque with increasing mineral oil concentrations. However, it was rather surprising to discover what appeared to be antiplasticization of the 128 000 and the 40 000 MW polystyrene blends even above T_g. With the 128 000 MW blends there was an increase in torque up to 4% mineral oil, followed by a decrease in torque at higher concentrations. In the case of the 40 000 MW blends, one observed that between 140 and 180 °C there was an increase in torque from 0 to 4.8% mineral oil followed by a decrease at 6%. Below 140 °C, the phenomenon was reversed. This behavior was confirmed in duplicate experiments. Furthermore, the activation energies for the 128 000 MW and 40 000 MW molecular weight polystyrene as shown in Table 2 were much higher than those typically observed for high molecular weight general-purpose polystyrenes (E_a = 12–22 kJ/mol).

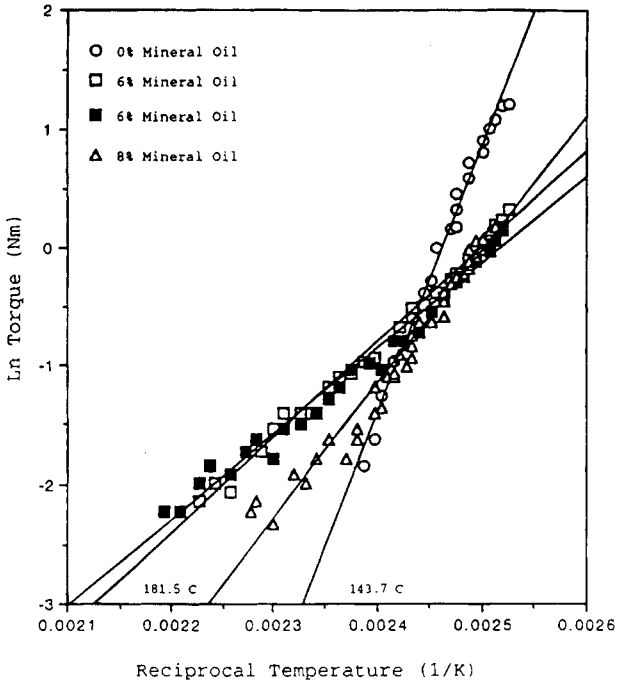

Figure 6. Effect of mineral oil concentration on torque of 40 000 MW blends.

Table 2. Activation Energies for the Polystyrene Blends

mol wt	mineral oil (vol %)	E_a (kJ/mol)
270 000	0	17
	6	20
	8	22
128 000	0	42
	2	40
	4	45
	8	39
40 000	0	188
	6	60
	6	67
	8	94

De Gennes found that the diffusion coefficient of a chain above T_g is inversely proportional to the square of the molecular weight and that the relaxation time is proportional to the cube of the molecular weight.[35] Doi and Edwards showed that viscosity is proportional to the cube of the molecular weight. This suggests that lower molecular weight polymers should relax at a faster rate than higher molecular weight polymers. Antiplasticization of the 40 000 and 128 000 MW polymers above and below T_g can be explained by shorter relaxation times of smaller molecules. In both temperature regimes, shorter chain lengths would exhibit higher frequency motions. Antiplasticization is manifested therefore by a slowing down of these faster motions.

Determination of Fractional Free Volume. Zoller et al. found that the specific volume of the polystyrene glass at 273 K was 0.9508 cm^3/g or 98.97 cm^3/mol.[37] According to Ougizawa et al., the equation of state parameters for polystyrene were independent of molecular weight above 34 000 Da.[38] Researchers at the Dow Chemical Co. found *PVT* data[39] for 200 000 and 300 000 molecular weight samples equivalent to Zoeller's data for 120 000 molecular weight materials. The Fox and Loshoek relationship also shows that the fractional free volume of polystyrene (a value of 0.116) is independent of the number-average molecular weight above 10 000 Da.[40] A comparison of ΔT_g values, i.e., $(T_{g\infty} - T_g)$, with Boyer's ΔT_g plots of $V-T$ data for thermal polystyrene fractions shows that a T_g of 63 °C for the 40 000 MW bimodal sample, hence a ΔT_g of 40 °C, corresponds to a "nominal" fractional free volume of about 0.112.[41]

Using eq 7, a value for α_g of 2.86×10^{-4} (°C^{-1}), and a value of 98.97 cm^3/mol for V_{273}K, the specific volume of polystyrene at 23 °C (296 K) was calculated to be 99.6 cm^3/mol. V_0, obtained from the literature, is 88.4 cm^3/mol.[41] Therefore the fractional free volume, f_v, is 0.112. This value is in agreement with the Simha–Boyer value of 0.113 derived empirically by relating the thermal coefficients of thermal expansion to the fractional free volume of a polymer glass.[41]

For the pure 40 000 MW polystyrene, τ_3 is 1.97 ns, which corresponds to an average hole diameter of 0.566 nm and an average hole volume, $\langle V \rangle$, of 0.095 nm^3 (eqs 1 and 2). The fraction of o-Ps intensity, I_3, is 0.453. Therefore the proportionally constant c as defined in eq 4 is 2.60 nm^{-3}. The number density of holes, N, is calculated to be 1.18 nm^{-3}, or one hole every 0.85 nm^3.

The number density of holes and fractional free volume of the blends were then determined using

$$N = 2.60 I_3 \tag{12}$$

$$f_V = 2.60 I_3 \langle V \rangle \tag{13}$$

Figure 7 shows the effect of mineral oil concentration on the o-Ps lifetimes (Figure 7a) and average hole sizes (Figure 7b) for the polystyrene blends. Mineral oil had no effect on the average hole size of the 270 000 MW blends. There was a slight increase in the average hole size of the 128 000 MW blends from 0.107 to 0.110 nm^3 with mineral oil addition. The lifetimes of the 40 000 MW blends increased steadily with increasing mineral oil concentration. This corresponds to an increase in the average hole volume from 0.095 to 0.101 nm^3. Apparently, in the case of the 128 000 MW and 40 000 MW blends, the mineral oil filled the smaller holes first. The remaining larger holes contributed to the increased average o-Ps lifetimes.

Figure 8 shows the effect of mineral oil concentration on the o-Ps intensities (Figure 8a) and number densities of holes (Figure 8b) for the polystyrene blends. The o-Ps intensities of the 270 000 MW blends remained constant. There was a 7% decrease in number density of holes for the 128 000 MW blend. With the 40 000 MW sample, the number of holes per unit volume decreased by 10% at the maximum degree of antiplasticization (6% mineral oil) and increased with higher levels of mineral oil.

Figure 9 shows that addition of 3.5% mineral oil caused a 3.6% decrease in fractional free volume in the 128 000 MW sample. There was a 9% decrease in fractional free volume at 6% mineral oil for the antiplasticized 40 000 MW polystyrene. There was no change in the free volume of the 270 000 MW sample, which was plasticized.

The PAS data suggest that in the 40 000 MW and 128 000 MW polystyrene the mineral oil filled the smaller holes at the chain ends first, leaving the larger holes along the polymer backbone relatively deficient in mineral oil. At higher mineral oil concentration, where phase separation of the mineral oil occurs, these larger holes become sufficiently filled to allow easier slippage between longer chain lengths, resulting in plasticization.

There is other evidence that the smaller holes are filled first. Researchers have observed a suppression and then disappearance of the T_β peak in antiplasticized materials.[14] According to Boyer, the β transition involves torsional or rotational motion of 1–3 monomer

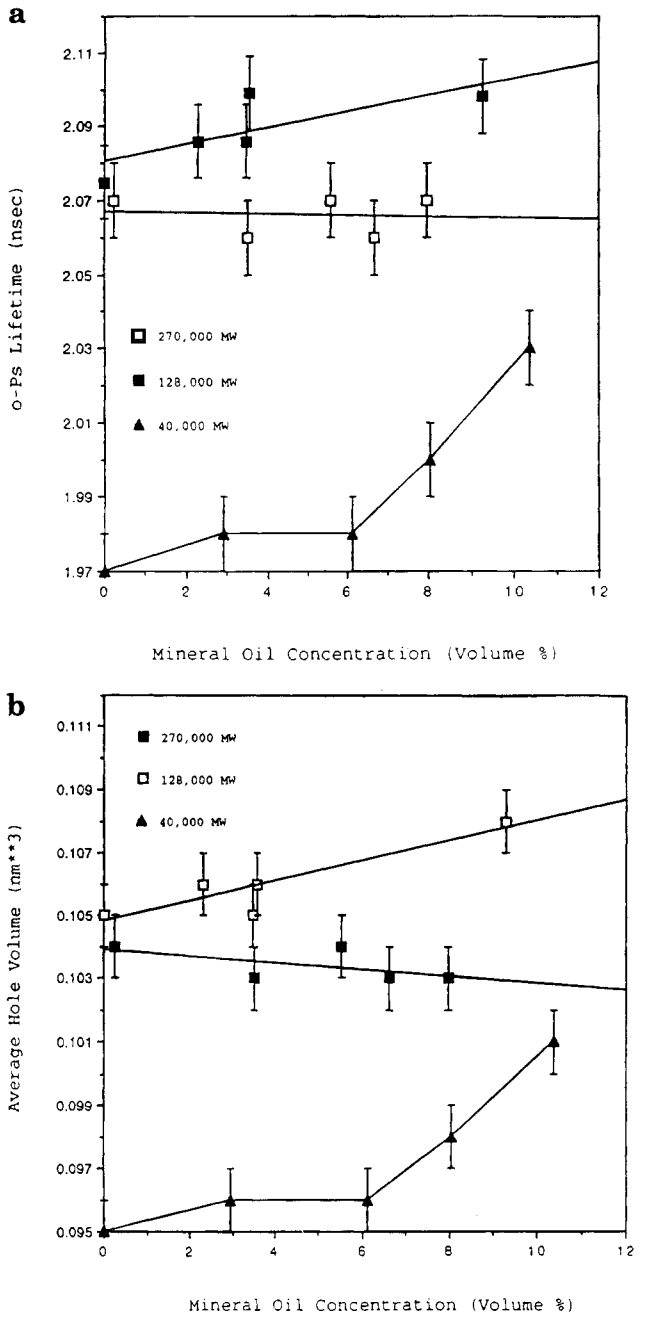

Figure 7. Effect of mineral oil concentration on (a) o-Ps lifetimes and (b) average hole sizes for polystyrene blends.

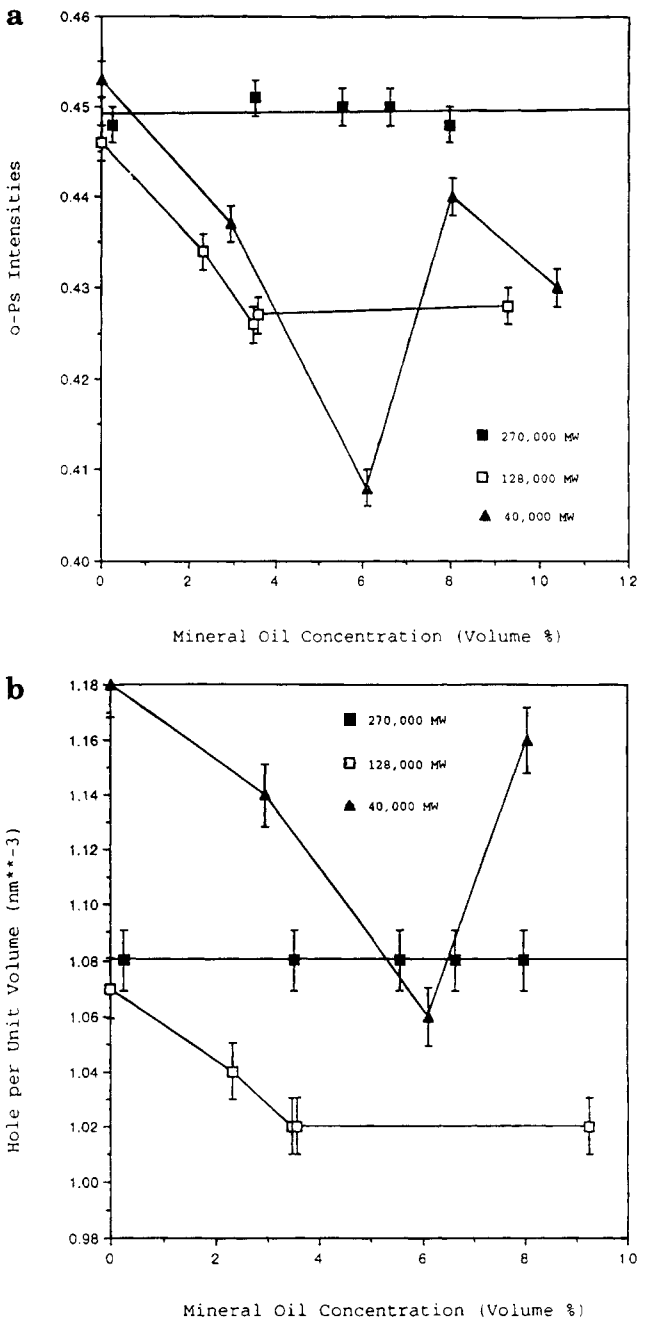

Figure 8. Effect of mineral oil concentration on (a) o-Ps intensities and (b) hole number densities for polystyrene blends.

repeat units or 1−10 consecutive atoms. Our argument is consistent with that of Boyer.[41] The β peak is suppressed and shifted to lower temperatures because the smaller holes are filled first.

Evidently, the mineral oil occupying voids at the chain ends contributed directly to antiplasticization, while the mineral oil residing along the polymer backbone was reponsible for the accompanying plasticization behavior observed. In the 270 000 MW polystyrene very few chain ends exist compared to the 128 000 MW and the 40 000 MW polystyrenes (a ratio of 1:2:83); thus a large proportion of the mineral oil will occupy voids along the polymer backbone. Those voids along the backbone are larger in volume than voids at the chain ends and hence never become sufficiently filled with mineral oil to effect antiplasticization.

The decrease in free volume in the 128 000 MW antiplasticized polystyrene was solely due to hole-filling by the mineral oil—blending 3.5 vol % mineral oil resulted in a 3.6% decrease in fractional free volume. However, in the case of the 40 000 MW sample, a 9% decrease in free volume was observed after blending with only 6% mineral oil. Perhaps, in addition to hole-filling by the mineral oil, the polymer may be realigning itself into a more densely packed state, thus causing a greater decrease in free volume than expected. It is thought that in blends that manifest antiplasticization, antiplasticization is dominant below a certain critical diluent level, whereas above that critical concentration, plasticization dominates.

^{13}C NMR and Chain Dynamics. Figure 10 shows the ^{13}C NMR spectrum of the 40 000 MW/6% mineral oil blend with peak assignments. The resonance positions are reported in terms of chemical shifts (ppm) with respect to tetramethylsilane (TMS). The backbone carbons were observed at 40 ppm. The methylene carbons on the backbone are sometimes distinguished

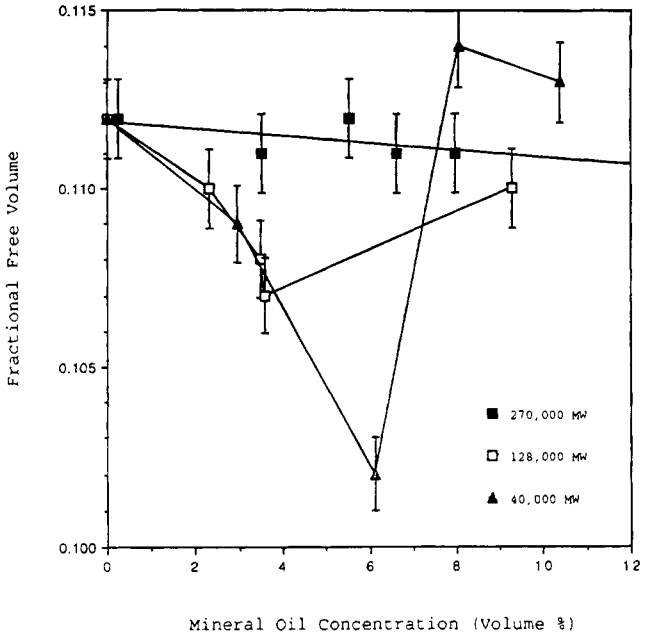

Figure 9. Effect of mineral oil concentration on fractional free volume of polystyrene blends.

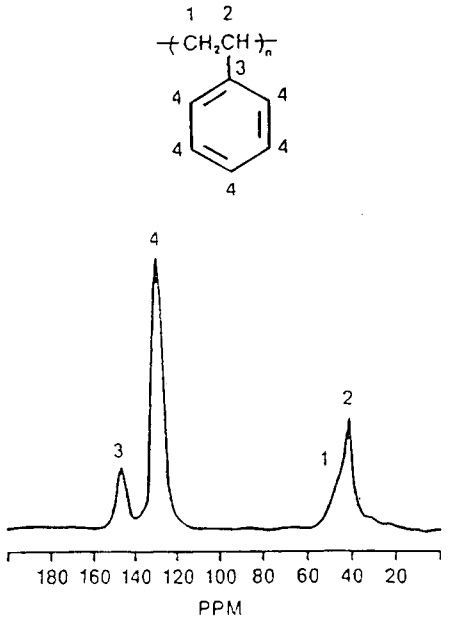

Figure 10. ^{13}C NMR spectrum of 6% 40 000 MW polystyrene blend.

as a shoulder at approximately 42 ppm. The quaternary carbon on the aromatic ring was observed at 145 ppm. The other five carbons on the aromatic ring show up as the intense signal at 127 ppm. Table 3 shows the results of the relaxation experiments of the 40 000 MW polystyrene/mineral oil blends in the rotating frame at room temperature. The relaxation times (ms) for the blends remain approximately the same as those of the

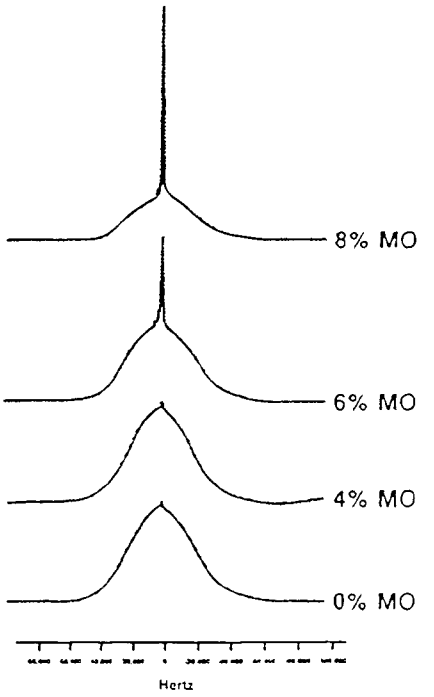

Figure 11. ^1H NMR spectra of 40 000 MW polystyrene blends.

virgin polymer regardless of whether the sample was antiplasticized (concentrations less than 6% mineral oil) or plasticized (6% or greater). These data imply that the mineral oil did not change the mobility of the polymer backbone, which supports our hypothesis of a chain end effect. It is believed that antiplasticization would affect the rate and/or amplitude of the chain end dynamics.

^1H NMR and Mineral Oil Domains. The ^1H NMR spectra of the 40 000 MW blends are shown in Figure 11. The sharp resonance peak at 1.6 ppm is due to mineral oil. As expected, no mineral oil peak was observed in the pure polystyrene sample. Although there was a sharp peak, attributable to mineral oil, in both the 6 and 8% blends, none was observed in the 4% blend. This indicates that at 4% the mineral oil was molecularly dissolved in the polystyrene.

The NMR data provide additional evidence that plasticization becomes dominant only at mineral oil concentrations greater than 6%—where phase separation of the mineral oil occurs.

Analysis of the ^1H NMR relaxation curves of the mineral oil peaks gave T_1 values of 0.5 and 1.5 s respectively for the 6 and 8% blends. Since in more mobile systems such as low-viscosity liquids, an increase in T_1, T_2, or $T_{1\varrho}$ indicates faster molecular motions, the higher T_1 values at 8% mineral oil indicate increased mobility of the mineral oil at higher concentrations as expected.

Table 4 shows the recovery factors as a function of spin-diffusion time for the 6 and 8% blends. The data are fitted to eq 9.

Table 3. NMR Spin–Lattice Relaxation Times (MS) for 40 000 MW Blends

	145 ppm			127 ppm			40 ppm		
% MO	T_{CH}	$T_{1\varrho}^H$	$T_{1\varrho}^C$	T_{CH}	$T_{1\varrho}^H$	$T_{1\varrho}^C$	T_{CH}	$T_{1\varrho}^H$	$T_{1\varrho}^C$
0	0.4	10.3	9.6	0.07	10.8	8.5	0.08	8.4	8.3
4	0.3	8.0	8.5	0.08	9.6	5.0	0.08	7.8	2.9
			9.1			5.9			3.6
6	0.3	11.5	9.6	0.08	10.7	8.6	0.09	8.8	7.1
			11.0			8.7			7.9
8	0.6	11.5	26.0	0.09	11.6	9.9	0.10	9.4	5.2
			36.0			10.6			5.2

Table 4. Recovery Factors as a Function of Diffusion Time

time (ms)	recovery factor: 6% mineral oil	recovery factor: 8% mineral oil
0.01	0.09	
0.02	0.18	
0.03	0.26	
0.04	0.33	
0.05	0.44	
0.06	0.48	
0.07	0.61	
0.08	0.67	
0.09	0.70	
0.10	0.74	
1.00		0.02
5.00		0.06
10.00		0.11
15.00		0.15
20.00		0.17
25.00		0.17
30.00		0.19
35.00		0.20
40.00		0.22

The domain size will now be calculated using the 6% blend as an example. T_2 can be determined from

$$T_2 = 1/(\pi\Delta l/2) \qquad (14)$$

where $\Delta l/2$ is the line width. The polystyrene line width was 34 kHz; thus T_2 was 9.4×10^{-6} s. D calculated from eq 10 was 5.6×10^{-12} cm^2/s. The value for D/b^2 determined by fitting the recovery factors to eq 9 was 12.17 ms^{-1} or 1.22×10^4 s^{-1}. Thus b was calculated to be 2.16×10^{-8} cm or 0.2 nm.

Fitting the 8% recovery factors in Table 4 to eq 9 yielded a value for D/b^2 of 0.00728 ms^{-1}. The domain size of the mineral oil in the 8% blends was calculated to be approximately 8.8 nm.

The ^{1}H NMR data confirmed that during the process of antiplasticization (less than 6% mineral oil) the mineral oil was intimately mixed with the polystyrene matrix. At concentrations above the solubility limit of the mineral oil, where phase separation occurred, plasticization was dominant.

Comparison of Mineral Domains and Free Volume Holes. Table 5 compares the average hole sizes obtained via PAS experiments in the 40 000 MW blends with the mineral oil domain sizes determined by NMR. At the critical domain size of about 9 nm (6% mineral oil) phase separation occurred and plasticization was dominant. The data show that at concentrations of greater than 6%, the size of mineral oil domains was 1 order of magnitude larger than the average size of the holes. Thus it can be deduced that antiplasticization is manifested only when the mineral domains approximate the average hole sizes.

Development of Antiplasticization Model. Table 6 compares the relative chain end concentrations (number of chain ends per nm^3) for the various polystyrene samples. The chain end concentration was calculated using the following equation:

$$\mathrm{CE} = (2/M_n)N_A\varrho \qquad (10^{-21}\ \mathrm{cm^3/nm^3}) \qquad (15)$$

where CE = chain end concentration (molecules/nm^3), M_n = number-average molecular weight, N_A = avogadro's number (6.023×10^{23}), and ϱ = density of polystyrene (g/cm^3). Table 6 shows that there was a significantly greater concentration of chain ends in the 40 000 MW sample than in the 270 000 MW sample—the ratio of chain end concentration was 83:1.

Table 5. Comparison of Mineral Oil Domains with Hole Sizes

% mineral oil	hole diameter from PAS (nm)	mineral domain from NMR (nm)
0	0.566	0
4	0.567	<0.2
6	0.568	0.2
8	0.572	8.8

Table 6. Comparison of Relative Chain End Densities

MW	M_n	chain end concn from PAS (mol/g)	bulk density (g/cm^3)	chain end density (number per nm^3)	ratio of chain end densities[a]
40 000	850 56 970	1.43×10^{-3}	1.058	0.911	83
128 000	58 420	3.42×10^{-5}	1.047	0.022	2
270 000	117 000	1.79×10^{-5}	1.047	0.011	1

[a] Ratio of chain end concentration in sample to that in 270 000 MW polystyrene.

Table 7. Free Volume Holes Associated with Chain Ends

MW	chain end density (number per nm^3)	total hole density (number per nm^3)	backbone hole density (number per nm^3)	% chain end holes
40 000	0.911	1.18	0.269	77.2
128 000	0.022	1.07	1.048	2.1
270 000	0.011	1.08	1.069	1.0

Table 8. Effect of Mineral Oil Concentration on Mineral Oil Domain Sizes in 40 000 MW Polystyrene Blends

% mineral oil	hole diameter (nm)	mineral oil domain (nm)	no. of MO molecules
0	0.566	0	0
4	0.567	<0.2	<1
6	0.568	0.2	1
8	0.572	8.8	357

Table 7 compares the relative number densities of holes. As molecular weight was increased, the total number densities of holes decreased. However, if one associates each chain end with a hole, then one can determine the number of holes not associated with the chain ends (backbone holes) from the difference between the total number density of holes and the concentration of chain ends. The table shows that as molecular weight increases, the number of backbone holes increases significantly. In other words, the percentage of the holes associated with the chain ends decreases as the molecular weight is increased. In the case of the 40 000 MW sample, 77% of the holes are associated with the chain ends. In the case of the 128 000 MW and 270 000 MW samples, 2 and 1% of the holes are associated with the chain ends, respectively.

Table 8 shows how the size and number of mineral oil molecules vary with the mineral oil concentration in the 40 000 MW blends. The mineral oil domains were calculated from Goldman–Shen NMR experiments as discussed earlier. GC experiments showed that the mineral oil consisted of primarily C-28 to C-46 straight-chain alkanes, with a nominal average of C-36. The volume of a C-36 alkane calculated using group contribution values is 605 cm^3/mol or 1 nm^3/molecule.[42] If one assumes spherical mineral oil domains, then the average diameter of a mineral oil molecule is 1.2 nm.

The Goldman–Shen technique measures the mobile mineral oil domain sizes. No mineral oil was detected at 4%. Thus is can be deduced that at 4% concentration, during antiplasticization, in addition to being intimately mixed with the polystyrene matrix, the mineral oil was

immobile in the chain end holes. Table 8 shows that at 6% the average size of the mineral oil domain determined by NMR was 0.2 nm. This represents the average of a distribution of domain sizes. At 6%, each mobile domain site represented less than 1% of a mineral oil molecule. As more mineral oil was blended into the polystyrene, phase separation, due to pooling of the mineral oil, occurred outside of the polymer chain end hole, resulting in a larger average domain size. This larger domain size is consistent with the earlier observations of higher T_1 values for the mineral oil, which reflected increased mobility of the mineral oil molecules at 8% concentration.

Arnould and Laurence's work suggests that the effective volume of mineral oil may be less than calculated.[43] At 6% no more than one mineral oil molecule was associated with each polymer chain end.

The question then becomes, How does the mineral oil molecule interact with the chain end hole? It is obvious that the volume of the mineral oil molecule (1 nm^3) is much larger than the average size of the holes (0.095 nm^3) in the 40 000 MW sample. Bendler claimed that the average free volume of polystyrene chain ends is 0.08 nm^3.[44] This is approximately 80% of the average size of the holes (0.095 nm^3) as determined from PAS experiments in this study. Earlier in this paper it was shown that 80% of the holes in the 40 000 MW sample are associated with the chain ends. It is reasonable to assume that the mineral oil molecule will enter the hole head first, i.e., with the CH_3 end. The volume of a CH_3 unit is 22.8 cm^3/mol or 0.038 nm^3/molecule, which results in a diameter of 0.42 nm.[42] Using the value of 80% of the average free volume of the holes (based on agreement with Bendler's data) gives a value of 0.076 nm^3, which corresponds to a diameter of 0.52 nm.

A comparison of the hole diameter of 0.52 nm with the diameter of a CH_3 unit (0.42 nm) suggests that each hole can accommodate the head of a mineral oil chain with the tail dangling outside. This supports the earlier deduction that each chain end has 1 mineral oil molecule associated with it during antiplasticization (i.e., at concentrations of 6% and less mineral oil). Conceivably, the chain end hole may be able to accommodate an additional mineral oil head through expansion. Since the polymer chain ends are relatively mobile compared to the polymer backbones, the chain end voids may fluctuate to fit additional mineral molecules. The chain ends are then compressed into a smaller volume, which can result in greater densification of the polymer than expected. For example, it was reported previously (Figure 8b) that there was a 10% decrease in free volume when 6% of mineral oil was added to the 40 000 MW polymer. The increased densification further restricts the mobility of the PS chain end, increases stiffness, and causes embrittlement.

The value of 0.42 nm for the diameter of the methyl end of the mineral oil molecule is also in agreement with Jackson and Caldwell's conclusions.[1,2] They stated that one necessary characteristic of an antiplasticizer is that it should have one dimension less than 0.55 nm.

In the 270 000 MW sample only 1% of the holes are associated with the chain ends. This means that 99% of the holes are along the polymer backbone, which is relatively rigid compared to the mobile chain ends. The small concentration of holes at the chain ends is not enough to effect any detectable or measurable antiplasticization. At low concentrations any mineral oil entering the larger holes does not quite fill the holes. Blending additional mineral oil into the 270 000 MW sample results in pooling or clustering of the mineral oil, which is then observed as haziness or phase separation in the PS blend. In fact, this phase separation of the mineral oil has been observed to be as low as 1% by other researchers using NMR techniques with 300 000 MW polystyrene blends containing mineral oil.[45]

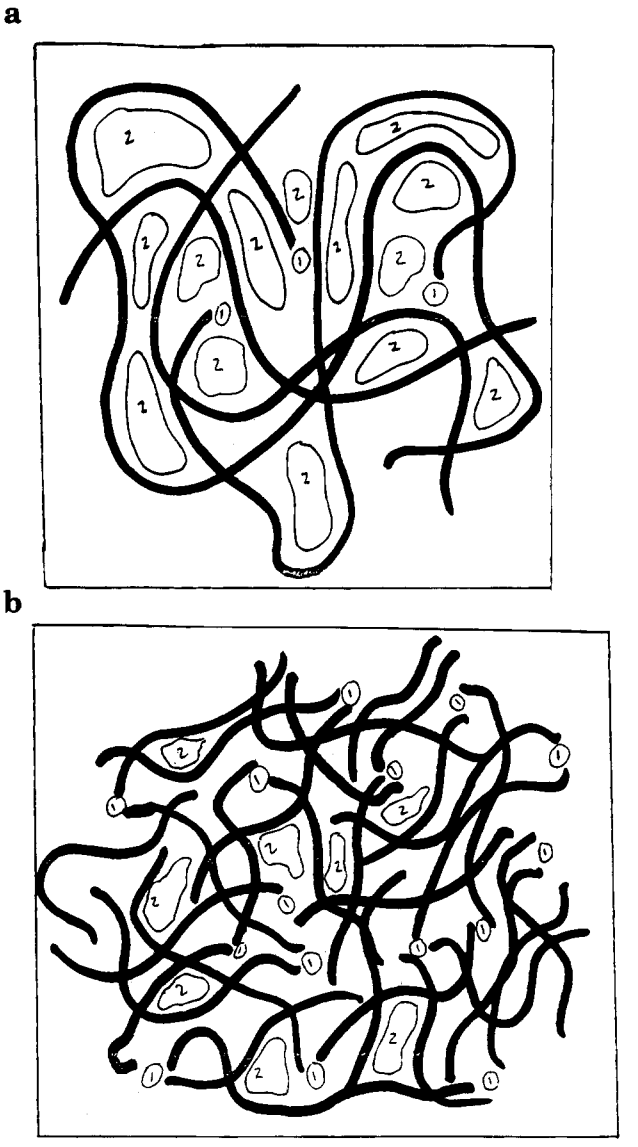

Figure 12. Schematic of (a) an amorphous high molecular weight polymer/diluent blend and (b) an amorphous low molecular weight polymer/diluent blend.

Model for Antiplasticization. Figure 12 shows schematics of amorphous polymers having very high (Figure 12a) and very low (Figure 12b) chain end concentrations. These figures are adaptations of the Flory random coil model.

When a diluent is blended into a polymer and the average size of the dispersed domains is less than or equal to the average diameter of the free volume voids, the diluent fills the smaller holes first at position 1. When larger quantities of diluent are added, the average domain size increases, and the diluent will occupy position 2 along the polymer backbone.

In a high molecular weight polystyrene sample (M_n = 100 000 Da) as shown in Figure 12a, about 1% of the free volume holes are associated with the chain ends compared to a low molecular weight sample (M_n = 1000 Da), as shown in Figure 12b, where approximately 80% of the free volume holes are associated with the chain ends. Thus in the high molecular weight sample, the effects of antiplasticization would not be measured. In

the low molecular weight sample, after the polymer chain end holes are filled, the effects of antiplasticization would be significant.

With a diluent such as mineral oil, the CH_3 end fills the hole at position 1. After the chain end holes are filled, as more mineral oil is added, clustering or pooling of the mineral oil occurs. The large difference (>0.9 (cal/cm^3)$^{0.5}$) in solubility parameters, 7.6 (cal/cm^3)$^{0.5}$ versus 9.1 (cal/cm^3)$^{0.5}$ for mineral oil and polystyrene, respectively, suggests stronger diluent–diluent attractive forces than polymer–diluent forces, leading to phase separation of the mineral oil.[46] Position 2 represents clustering of the diluent at high concentrations, where phase separation occurs. In polymers where there is significant main-chain mobility, such as polycarbonate, diluent occupation of positions 2 may lead to antiplasticization. In fact, Cais et al. have observed antiplasticization in polycarbonate blends containing as much as 40 wt % diluent.[16] They speculated that antiplasticization at these high diluent concentrations may be due to interaction between the diluent molecules and the polymer backbone. This interaction would in turn restrict mobility of the main-chain segments.

Conclusions

Antiplasticization in polymers is molecular weight dependent and diluent concentration dependent. These results support a hypothesis that the phenomenon can be attributed to a chain end effect. There was a decrease in fractional free volume of antiplasticized blends (PAS data), while there was no change in the polymer backbone dynamics (^{13}C NMR data). Antiplasticization occurs when the average diameter of the mineral oil domains approximates the average size of the free volume voids (^{1}H NMR Goldman–Shen data). One mineral oil molecule was associated with each chain end during antiplasticization. At concentrations above the solubility limit of the mineral oil, where the mineral oil domain sizes are significantly larger than the average free volume hole diameter, phase separation occurs, and plasticization is dominant. The PAS and NMR results are consistent with the hypothesis that antiplasticization is due to a decrease in fractional free volume at the chain ends. The diluent initially fills the smaller holes at the chain ends. Mobility of the chain ends is restricted and thus results in higher moduli and strength, which is usually accompanied by embrittlement of the polymer.

Acknowledgment. The authors gratefully acknowledge the financial support from the Designed Thermoplastics Research Laboratory and the Analytical Sciences Laboratory of The Dow Chemical Co., this being the result of the first industrial–Ph.D. joint venture with the Department of Chemical Engineering at Michigan State University. In addition, the majority of this work would not have been accomplished without the generous assistance from several individuals at The Dow Chemical Co.

References and Notes

(1) Jackson, W. J., Jr.; Caldwell, J. R. *J. Appl. Polym. Sci.* **1967**, *11*, 211.
(2) Jackson, W. J., Jr.; Caldwell, J. R. *J. Appl. Polym. Sci.* **1967**, *11*, 227.
(3) Maeda, Y.; Paul, D. R. *J. Polym. Sci., Part B: Polym. Phys.* **1987**, *25*, 1005.
(4) Vrentas, J. S.; Ling, H. C.; Duda, J. L. *Macromolecules* **1988**, *21*, 1470.
(5) Roy, A. K.; Inglefield, P. T.; Shibata, J. H.; Jones, A. A. *Macromolecules* **1987**, *20*, 1434.
(6) Lui, Y.; Roy, A. K.; Jones, A. A.; Inglefield, P. T.; Ogden, P. *Macromolecules* **1990**, *23*, 968.
(7) Maeda, Y.; Paul, D. R. *Polymer* **1985**, *28*, 2055.
(8) DeLassus, P. T. Diffusion, Styrene Polymers. In *Encyclopedia of Polymer Science and Engineering*; John Wiley and Sons: New York, 1989; Chapter 16, p 165.
(9) Kinjo, N.; Kakagawa, T. *Polym. J.* **1973**, *4*, 143.
(10) Makaruk, L.; Polanski, H.; Mizerski, T. *J. Appl. Polym. Sci.* **1979**, *23*, 1935.
(11) Belfiore, L.; Cooper, S. L. *J. Polym. Sci., Polym. Phys. Ed.* **1983**, *21*, 2135.
(12) Sefcik, M. D.; Schaefer, J.; May, F. L.; Raucher, D.; Dub, S. M. *J. Polym. Sci., Polym. Phys. Ed.* **1983**, *21*, 1041.
(13) Deshpande, D. D.; Kandaswamy, N. R.; Tiwari, V. K. *J. Appl. Polym. Sci.* **1985**, *30*, 2869.
(14) Dumais, J. J.; Cholli, A. L.; Jelinski, L. W.; Hedrick, J. L.; McGrath, J. E. *Macromolecules* **1986**, *19*, 1884.
(15) Guerrero, S. J. *Macromolecules* **1989**, *22*, 3480.
(16) Cais, R. E.; Nozomi, M.; Kawai, M.; Miyaki, A. *Macromolecules* **1992**, *25*, 4588.
(17) ASTM Standard Test Methods for Flexural Properties of Plastics and Electrical Insulating Materials, ASTM D790.
(18) Shah, V. *Handbook of Plastics Testing Technology*; John Wiley and Sons: New York, 1984; p 23.
(19) Baijal, M. D. *Plastics Polymer Science and Technology*; John Wiley and Sons: New York, 1982; p 809.
(20) Jean, Y. C.; Schrader, D. M. Experimental Techniques in Positron and Positronium Chemistry. In *Positron and Positronium Chemistry*; Elsevier: New York, 1988; Chapter 3.
(21) Tao, S. J. *J. Chem. Phys.* **1972**, *56*, 5499.
(22) Nakanishi, H.; Wang, S. J.; Jean, Y. C. *Proceedings of the International Conference on Positron Annihilation in Fluids, Arlington, TX*; Sharma, S. C., Ed.; World Scientific Publishing: Singapore, 1987; p 292.
(23) Brandt, W.; Berko, S.; Walker, W. W. *Phys. Rev.* **1960**, *120*, 1289.
(24) Bondi, A. *J. Polym. Sci.* **1964**, *A2*, 3159.
(25) Becker, E. D. *High Resolution NMR Theory and Chemical Applications*; Academic Press, Inc.: New York, 1984.
(26) Gerstein, B. C.; Dybowski, C. R. *Transient Techniques in NMR of Solids*; Academic Press: London, 1985.
(27) Schaefer, J.; Stejskal, E. In *Topics in Carbon-13 NMR Spectroscopy*; Wiley: New York, 1979; Vol. 3, Chapter 4.
(28) Schaefer, J.; Stejskal, E. O.; Steger, T. R.; Sefcik, M. D.; McKay, R. A. *Macromolecules* **1980**, *13*, 1121.
(29) Goldman, M.; Shen, L. *Phys. Rev.* **1966**, *144*, 321.
(30) Cheung, T. T. P.; Gerstein, B. C. *J. Appl. Phys.* **1981**, *52*, 5517.
(31) Kirkegard, P.; Eldrup, M. *Comput. Phys. Commun.* **1984**, *7*, 401.
(32) Braun, G.; Kovacs, A. J. *C. R. Acad. Sci.* **1965**, *260*, 2217.
(33) Pezzin, G.; Omacini, A.; Zilio-Grandi, F. *Chim. Ind.* **1968**, *50*, 309.
(34) Boyer, R. Transitions and Relaxations in Amorphous and Semicrystalline Organic Polymers and Copolymers. In *Encyclopedia of Polymer Science and Technology*; John Wiley and Sons, Inc: New York, 1977; Supplement, Vol. II, p 797.
(35) De Gennes, P.-G. *J. Chem. Phys.* **1971**, *55*, 572.
(36) Doi, M.; Edwards, S. F. *The Theory of Polymer Dynamics*; International Series of Monographs on Physics–73; Oxford University Press: New York, 1989; p 191.
(37) Zoller, P.; Hoehn, H. H. *J. Polym. Sci., Polym. Phys. Ed.* **1982**, *20*, 1385.
(38) Ougizawa, T.; Dee, G. T.; Walsh, D. J. *Polymer* **1989**, *30*, 1675.
(39) Whiting, L. F. The Dow Chemical Co., personal communication, 1991.
(40) Fox, T. G., Jr.; Loeshek, S. *J. Polym. Sci.* **1955**, *15*, 371.
(41) Boyer, R. Transitions and Relaxations in Amorphous and Semicrystalline Organic Polymers and Copolymers. In *Encyclopedia of Polymer Science and Technology*; John Wiley and Sons, Inc: New York, 1977; Supplement, Vol. II, p 761.
(42) Van Krevelen, D. W.; Hoftyzer, P. J. *Properties of Polymers*; Elsevier: New York, 1976; Chapter 4.
(43) Arnould, D.; Laurence, R. L. *Ind. Eng. Chem. Res.* **1992**, *31*, 218.
(44) Bendler, J. T. Transitions and Relaxations. In *Encyclopedia of Polymer Science and Engineering*; Wiley: New York, 1989.
(45) Smith, P. J.; Ellaboudy, A. S. The Dow Chemical Co., personal communication, 1992.
(46) Grulke, E. A. Solubility Parameter Values. *Polymer Handbook*; Wiley: New York, 1989.

MA945072N